Clinical impact of copy number variation changes in bladder cancer samples

VICTORIA SPASOVA[1], BORIS MLADENOV[2], SIMEON RANGELOV[3], ZORA HAMMOUDEH[1], DESISLAVA NESHEVA[1], DIMITAR SERBEZOV[1], RADA STANEVA[1,4], SAVINA HADJIDEKOVA[1,4], MIHAIL GANEV[1], LUBOMIR BALABANSKI[1,5], RADOSLAVA VAZHAROVA[5,6], CHAVDAR SLAVOV[3], DRAGA TONCHEVA[1] and OLGA ANTONOVA[1]

[1]Department of Medical Genetics, Medical University-Sofia, 1431 Sofia; [2]Department of Urology, UMBALSM N.I. Pirogov, 1606 Sofia; [3]Department of Urology, Tsaritsa Yoanna University Hospital, 1527 Sofia; [4]Medical Genetics Laboratory, Nadezhda Women's Health Hospital, 1373 Sofia; [5]Medical Genetics Laboratory, GARH Malinov, 1680 Sofia; [6]Department of Biology, Medical Genetics and Microbiology, Faculty of Medicine, Sofia University St. Kliment Ohridski, 1407 Sofia, Bulgaria

Received November 30, 2019; Accepted February 18, 2021

DOI: 10.3892/etm.2021.10333

Abstract. The aim of the present study was to detect copy number variations (CNVs) related to tumour progression and metastasis of urothelial carcinoma through whole-genome scanning. A total of 30 bladder cancer samples staged from pTa to pT4 were included in the study. DNA was extracted from freshly frozen tissue via standard phenol-chloroform extraction and CNV analysis was performed on two alternative platforms (CytoChip Oligo aCGH, 4x44K and Infinium OncoArray-500K BeadChip; Illumina, Inc.). Data were analysed with BlueFuse Multi software and Karyostudio, respectively. The results highlight the role of genomic imbalances in regions containing genes with metastatic and proliferative potential for tumour invasion. A high level of genomic instability in uroepithelial tumours was observed and a total of 524 aberrations, including 175 losses and 349 gains, were identified. The most prevalent genetic imbalances affected the following regions: 1p, 1q, 2q, 4p, 4q, 5p, 5q, 6p, 6q, 7q, 8q, 9p, 9q, 10p, 10q, 11q, 13q and 17q. High-grade tumours more frequently harboured genomic imbalances (n=227) than low-grade tumours (n=103). A total of 36 CNVs in high-grade bladder tumours were detected in chromosomes 1-5, 8-11, 14, 17, 19 and 20. Furthermore, five loss of heterozygosity variants containing 176 genes were observed in high-grade bladder cancer and may be used as potential targets for precision therapy. Revealing specific chromosomal regions related to the metastatic potential of uroepithelial tumours may lay a foundation for implementing molecular CNV profiling of bladder tumours as part of a routine progression risk estimation strategy, thus expanding the personalized therapeutic approach.

Correspondence to: Dr Olga Antonova, Department of Medical Genetics, Medical University-Sofia, 2 Zdrave Street, 1431 Sofia, Bulgaria
E-mail: olga_boyanova@yahoo.com

Key words: bladder, cancer, metastasis, invasion, copy number variations, loss of heterozygosity

Introduction

The most successful approach to treating a disease has always been etiological therapy. In the case of bladder cancer, however, this approach remains inapplicable, as the mechanism of disease development has remained to be fully elucidated. Over 90% of bladder tumours are transitional cell carcinomas - frequently recurrent, but mostly non-invasive. However, they are a heterogeneous group with at least two distinct subgroups with different clinicopathological features-low-grade, non-infiltrating cancers and high-grade, muscle-invasive cancers (1). In addition, based on their clinical behavior, non-infiltrating tumours are subdivided into non-progressive (70%) and progressive types (10-20%), whereas high-grade, muscle-invasive cancers are subdivided into ones with a relatively good prognosis and those with a poor prognosis with a five-year survival rate of <50% (2). It is required to improve the current knowledge on this clinical diversity and the specific molecular mechanisms that underlie this variation in tumour behaviour.

Over 20% of non-invasive bladder tumours have been indicated to have genomic imbalances, including losses in the short (p) and long (q) chromosomal arm: 11p, 11q, 8p, 9, 17p, 3p and 12q and gains in the 8q21, 13q21-q34, 1q31, 3q24-q26 and 1p22 chromosomes (3). Deletions in the chromosomal regions 2q, 3p, 4p, 4q, 5q, 6q, 8p, 9p, 9q, 10q, 11p, 13q, 17p, 18q and Y and duplications/gains in 1q, 3q, 8q, 11q13, 17q and 20q and chromosome 7 are frequently detected (3-6).

In comparison, copy number variations are reported in 30% of invasive bladder tumours, including elevated copy number in the 1q23-24 chromosomal region, deletions in the 2q, 4q, 5p, 6q, 9p21.3, 8p23.1, 10p, 10q, 11p13 and 18q, as well

as duplications in the 6p22, 8p12, 8q22, 11q13, 19q13 and 20q regions (7). In 2003, Veltman *et al* (8) reported significant correlations between copy number gain of *CCNE1*-containing regions and gain of *ERBB2*, as well as a correlation between copy number gain of *CCND1* and deletion of *TP53*. So far, no interdependence has been established between CNV findings and tumour stage or grade.

Most of the studies related to quantitative genomic changes were performed with low-resolution comparative genomic hybridization (CGH). Studies on DNA imbalances in bladder cancer performed using high-resolution microarray-based CGH (aCGH) provided comprehensive information on quantitative genomic changes, but due to the small sample size (usually between 7 and 40 bladder cancer samples), they lacked statistical power (1,9-11). The situation with expression microarray studies, which focused on detecting changes in gene expression levels or mRNA levels, is similar (12-15). Despite the promising results from these studies, the current understanding of the mechanisms involved in the progression of bladder tumours remains insufficient. Advances in molecular methods allowing for high-resolution locus-by-locus detection of CNVs may possibly improve the understanding of the molecular pathology of bladder cancer progression and facilitate the discovery of novel drug targets and therapeutic approaches (16).

The aim of the present pilot study was to detect CNVs related to tumour progression and metastasis of urothelial carcinoma through whole-genome CNV scans of fresh frozen samples.

Materials and methods

Ethics. This study was approved by the Ethical Committee of the Medical University of Sofia (Sofia, Bulgaria; protocol No. 04/09/03/2018). Written informed consent and a questionnaire on family history, as well as professional and environmental health hazards, were obtained from all participants prior to tissue collection.

Bladder cancer samples. A total of 30 bladder cancer samples from 6 females and 24 males were collected for the present study. Samples were collected for 12 months (January 2018 to January 2019) at the Department of Urology, UMBALSM N.I. Pirogov and Department of Urology, Tsaritsa Yoanna University Hospital. The clinical and pathological characteristics of the studied cohort are described according to the age of the patients, sex, smoking habits, professional risk factors, tumor stage and grade (Table I).

aCGH. The samples were transported in sterile containers at 4˚C to the genetic laboratory, where DNA was extracted using a standard phenol-chloroform extraction protocol and stored at -20˚C. Isolated DNA was quantitatively assessed spectrophotometrically (NanoDrop® ND-2000c; Thermo Fisher Scientific, Inc.) and qualitatively by horizontal low-voltage agarose gel electrophoresis (Horizon 20-25; GibcoBRL; Thermo Fisher Scientific, Inc.).

Two independent platforms were used for the detection of genomic imbalances: i) CytoChip ISCA 4x44K v1.0 (BlueGnome), scanned with an Agilent G2505 microarray scanner (Agilent Technologies, Inc.) and analysed by BlueFuse Multi v3.1 (Illumina, Inc.) and ii) Infinium OncoArray-500K BeadChip (Illumina, Inc.), scanned with iScan (Illumina, Inc.) and analysed using KaryoStudio v.1.4 (Illumina, Inc.).

A total of 20 bladder cancer samples were analysed with the OncoArray-500K BeadChip, 12 cancer samples were analysed with the CytoChip ISCA 4x44K v1.0 and two tumour samples were analysed using both methods to confirm the robustness of the results.

All procedures, including sample preparation, sample processing, hybridization, scanning and data analysis, were performed using the manufacturers' standard protocols.

Genotype/phenotype interrelation. The interconnection between the genomic alterations and the clinical phenotype of tumours was assessed by a detailed analysis of publicly available databases such as the Database of Genomic Variants (DGV; http://projects.tcag.ca/variation/) and the Catalogue of Somatic Mutations in Cancer (Cosmic; https://cancer.sanger.ac.uk/cosmic).

Results

Bladder cancer samples. The clinical and pathological characteristics of the cohort are described in Table I and Fig. 1. The individual data for each case are presented in Table SI. The mean age of the studied patients was 67.77±9.3 years. A total of 46.7% of patients were smokers, with an average cigarette consumption of 16.9±6.19 per day. Four patients (13.3%) had professional risk factors related to the transport, oil and chemical industries.

CNV analysis. A total of two of the studied samples exhibited copy number changes in >70% of the genome. Therefore, they did not meet the qualitative criteria of the platform used and were excluded from any further analysis. Data from the remaining 28 samples were included in the next analytical steps. A total of 524 aberrations, including 175 losses and 349 gains, were detected (Table II).

According to the tumour stage, the aberrations were distributed as follows: Ta, n=64 (12.2%); T1, n=64 (12.2%); T2, n=334 (63.7%); T3, n=49 (9.4); and T4, n=13 (2.5%). The mean number of aberrations per tumour was as follows: Ta, 16 (range, 0-44); T1, 9 (range, 0-19); T2, 25.7 (range, 0-70); T3, 16.3 (range, 13-24); and T4, 13 (only one sample). Additionally, the number of aberrations were the highest for T2-stage tumours and the lowest for T1-stage tumours (Tables II and SII)

Detected aberrations were distributed according to tumour grade as follows: 19.7% (n=103) in G1 tumours, 37% (n=194) in G2 and 43.3% (n= 227) in G3 tumours. The total number of aberrations in G3 tumours was more than twice as high as that in tumours of the lowest grade G1, but the average number of aberrations per tumour was similar in the different tumour classes, with 14.7 aberrations in G1 (range, 1-45), 21.5 in G2 (range, 0-91) and 18.9 in G3 (range, 0-37) (Tables II and SII).

Only 10.7% (n=3) of the 28 cancer samples carried no chromosomal aberrations. The remaining 89.3% (n=25) displayed multiple chromosomal copy number changes. Of all imbalances, 396 (75.6%) were located in autosomal chromosomes. Autosomal chromosomal regions were

Table I. Summary of the clinical and pathological characteristics of patients with bladder cancer used in the present study.

Parameter	Value
Mean age	67.5±9.38 years
Smoking	14 (46.7%)
Cigarette consumption per day	16.6±6.19
Professional risk factors	4 (13.3%)
MMC therapy	4 (13.3%)
BCG therapy	1 (3.3%)
Grade	
G1	9 (30%)
G2	9 (30%)
G3	12 (40%)
Recurrence	
Recurrent	17 (56.7%)
Primary	13 (43.3%)
Lymph Node Metastasis	
Present	2 (6.7%)
Absent	28 (93.3%)

BCG, bacillus Calmette-Guérin; MMC, mitomycin C. All the categories are presented as mean values. Only the mean age and cigarette consumption per day parameters are presented as the mean ± SD.

Table II. Total number of detected CNVs (loss and gain) distributed by tumor stage and grade.

Aberrations	Tumor samples distributed by T and G	Detect CNVs distributed by T and G	Aberrations per tumor
pTa loss	4	20	5
pT1 loss	7	40	5.7
pT2 loss	13	78	6
pT3 loss	3	30	10
pT4 loss	1	7	7
pTa gain	4	44	10.7
pT1 gain	7	24	3.3
pT2 gain	13	256	19.2
pT3 gain	3	19	5.7
pT4 gain	1	6	6
G1 loss	7	41	5.8
G2 loss	9	61	6.8
G3 loss	12	73	6.1
G1 gain	7	62	8.8
G2 gain	9	133	14.8
G3 gain	12	154	12.8

CNVs, copy number variations; T, tumor stage; G, grade.

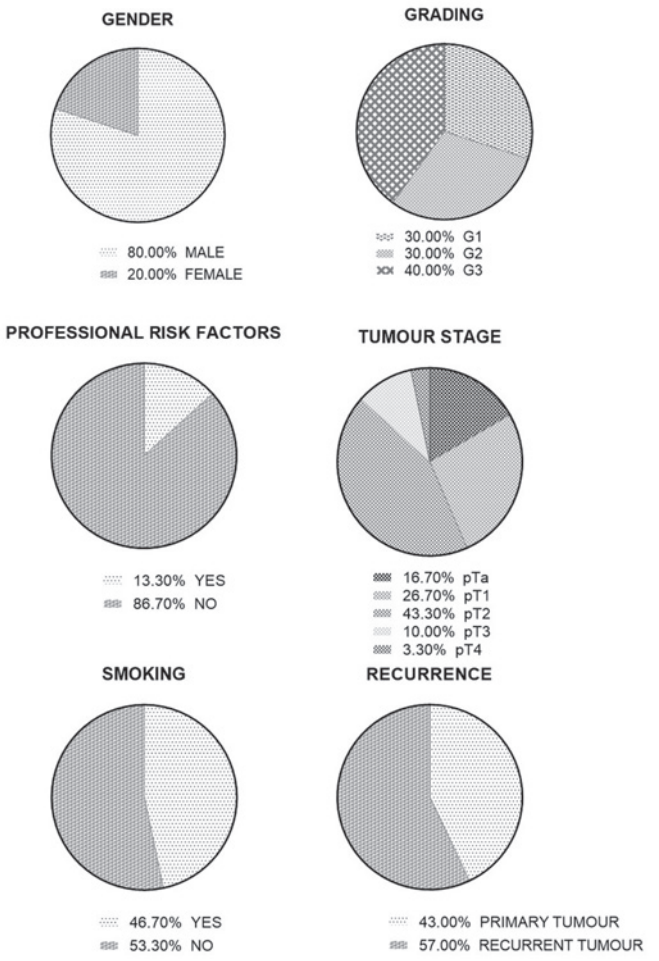

Figure 1. Characteristics of the patient cohort with pie charts displaying the distribution of the patients according to gender, professional health risk factors, tobacco smoking, tumour stage, grade and recurrence.

classified based on the number of detected imbalances as follows: i) Group 1 (0-5 CNVs detected), representing 7 chromosomal regions that harboured 6.3% (n=25) of all genomic imbalances, with 21q (n=1), 12p (n=2), 12q (n=4), 16p (n=4), 16q (n=4), 11p (n=5) and 18p (n=5); ii) Group 2 (6-9 CNVs detected), representing 14 chromosomal regions that harbour 27% (n=107) of all genomic imbalances, with 2p (n=8), 3p (n=7), 3q (n=7), 7p (n=7), 8p (n=8), 14q (n=9), 15q (n=6), 17p (n=7), 18q (n=8), 19p (n=6), 19q (n=9), 20p (n=8), 20q (n=9) and 22q (n=8); iii) Group 3 (≥10 CNVs detected), representing the remaining 18 autosomal chromosomal regions harbouring 66.7% (n=264) of all genomic imbalances, with 1p (n=12), 1q (n=16), 2q (n=15), 4p (n=11), 4q (n=16), 5p (n=10), 5q (n=18), 6p (n=23), 6q (n=13), 7q (n=10), 8q (n=12), 9p (n=25), 9q (n=23), 10p (n=13), 10q (n=10), 11q (n=13), 13q (n=10) and 17q (n=14) (Table SII). Chromosome 9 was the most severely affected, displaying 25 CNVs in the short arm and 23 in the long chromosomal arm, which accounted for 12.1% of all autosomal aberrations.

The share of sex chromosomal imbalances stood at 24.4% (n=128). The highest frequency of CNVs per chromosome was detected in the sex chromosomes, with 49 in the X (both losses and gains) and 79 in the Y chromosome (only losses - partial or complete) (Table SII).

Among the autosomal chromosomal regions with a high number of CNVs (≥10) (n=264), 79.9% of variations (n=211)

Table III. LOH regions detected in the bladder cancer samples.

Stage	Grade	Chr.	Cytoband	Start	End	Length in bp
T2	G2	6	p12.1-p11.1	55721511	58767335	3045824
T2	G2	7	q21.3	94372640	97676259	3303619
T2	G2	7	q22.1q22.2	99552168	104336782	4784614
T2	G3	11	q14.1q14.2	81417643	86071005	4653362
T2	G3	17	q25.1-q25.3	73593574	77382564	3788990

Chr., chromosome; LOH, loss of heterozygosity.

were chromosomal gains, while 20.1% (n=53) were losses. Five copy-neutral aberrations (LOH variants) were detected (Table III). Furthermore, 19.7% (n=52) of the copy number changes were <800 kB, frequently reported in DGV as polymorphic findings, so they were classified as 'benign'. Of the remaining CNVs, 76.1% (n=201) were labelled as pathogenic and 4.2% (n=11) were classified as variants with uncertain significance. According to the tumour stage, the aberrations were distributed in the following way: Ta, n=25; T1, n=30; T2, n=191; T3, n=1; and T4, n=6. According to the tumour grade, the majority of aberrations were present in G2-grade tumours and were distributed as follows: G1, n=40 (15.15%); G2, n=122 (46.21%); and G3, n=102 (38.64%) (Table SII).

Among the pathogenic gains, 16.04 (n=45) had overlapping regions in at least four different tumour samples, mostly high-grade: Chromosome 1, five regions (Fig. 2A, Table IV); chromosome 2, two regions (Fig. 2B, Table IV); chromosome 3, one region (Fig. 3A, Table IV); chromosome 4, two regions (Fig. 3B, Table IV); chromosome 5, two regions (Fig. 4A, Table IV); chromosome 8, four regions (Fig. 4B, Table IV). In chromosome 9, four overlapping chromosomal regions were detected, with both gains and losses (Fig. 5A, Table IV). Furthermore, the following overlapping regions were detected: Chromosome 10, two regions (Fig. 5B, Table IV); chromosome 11, one region (Fig. 6A, Table IV); chromosome 14, four regions (Fig. 6B, Table IV); chromosome 17, seven regions (Fig. 7A, Table IV); chromosome 19, two regions (Fig. 7B, Table IV); and chromosome 20, five regions (Fig. 7C, Table IV). The results obtained from the follow-up analysis of genes from the pathogenic gain regions are presented in Table V. This table includes genes related to cancer treatment, resistance, initiation, cell-cycle deregulation, tumor progression and metastases.

Comparison between the two CNV detection platforms. The two samples analysed with both platforms demonstrated no difference in the detected chromosomal abnormalities. Due to the higher resolution of the Infinium OncoArray-500K BeadChip (Illumina, Inc.), the coordinates of the detected aberrations were mapped comparatively more precisely. The region arr16q23.1q24 (74356681-88675439)x1, designated as one region by CytoChip ISCA 4x44K v1.0, was recognized as two regions, namely arr16q23.1(74500123-75740477) x1 and arr16q23.1 (75766088-77151891)x0, by the Infinium OncoArray-500K BeadChip. The latter platform detected an additional chromosomal region, arr16p12.1p11 (24577766-35173765)x3, which was below the resolution of the CytoChip ISCA 4x44K v1.0 arrays. Only the design of the Infinium OncoArray-500K BeadChip allowed for the detection of LOH regions.

LOH variants. Among the 19 tumour samples analysed with the Infinium OncoArray-500K BeadChip, five LOH variants were detected in chromosomes 6, 7, 11 and 17 Table V. These variants contained 176 genes (Table SIII).

Discussion

In the present study, a CNV analysis of 30 bladder cancer samples was performed. Despite the small number of patients in the present cohort, the epidemiological data obtained demonstrated the role of external hazardous factors in the development of bladder cancer. More than 46% of patients demonstrated unhealthy smoking habits and 13.3% had professional risk factors. These findings are consistent with results of previously conducted larger studies (17).

The high number of detected CNVs testifies the high level of genomic instability observed in both high-grade tumours (G3) and low-grade tumours (G1), and is in concordance with results of previous studies (1). The results obtained with regard to the role of Y-chromosome imbalances in bladder cancer were consistent with the insight gained in a study that demonstrated a strong tendency of Y-chromosome loss (18), but were partially in contrast to the studies of Conconi *et al* (1) from 2014 and Panani and Roussos (19) from 2006, where Y-chromosome amplification was detected. Due to the small size of the Y chromosome, the phenomenon of age-related loss of the Y chromosome and the development of bladder cancer in adulthood (20), it may be assumed that the loss of the Y chromosome in bladder cancer is a non-specific phenomenon.

A high number of genes related to cancer treatment, resistance, initiation and cell-cycle deregulation were located in the regions with pathogenic gains. Genes related to invasion and metastasis, in line with the aims of the present study, were the focus of the consequent data analysis. These genes are discussed below.

In tree CNV regions in chromosome 9, both losses and gains were detected: arr9p24.2p24.1 (4483189-7324382) x1, arr9p24.2p24.1 (4483189-7324382)x3 arr9p21.3 (21746274-22004153)x1, arr9p21.3 (21746274-22004153) x3, arr9q21.33q22.32 (89345014-96677307)x1 and

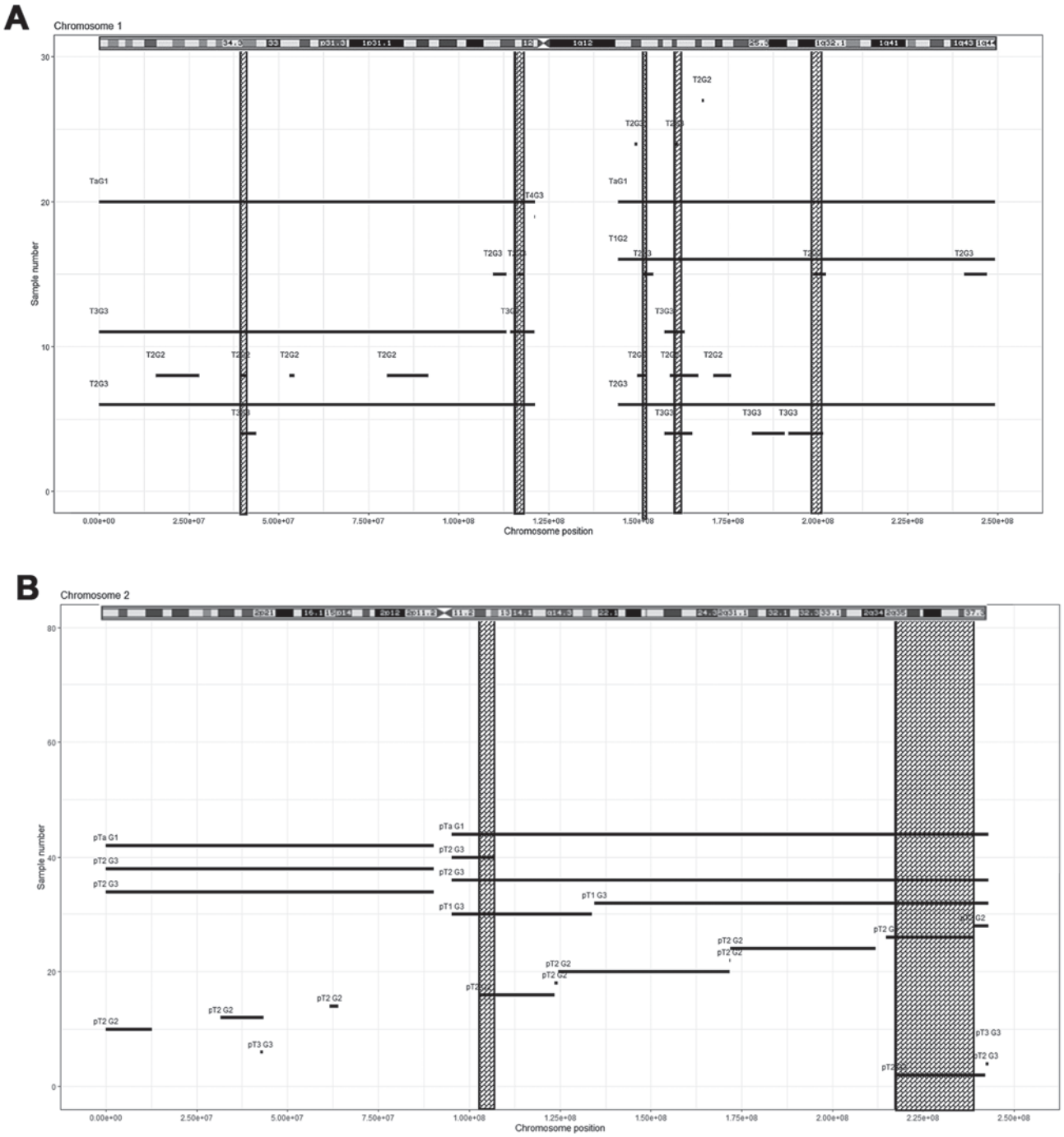

Figure 2. CNVs detected in (A) chromosome 1 and (B) chromosome 2. X-axis indicates the genomic position and the Y-axis indicates individual tumour samples tested. Chromosomal regions with a gain are indicated with a black straight line. No losses were detected. The shaded vertical fields indicate the start and the end of each CNV overlapping in at least five tumours. CNV, copy number variation.

arr9q21.33q22.32 (89345014-96677307)x3. These could be unspecific events due to high level of genomic instability in those regions. In the fourth region of chromosome 9, arr9q 33.3q34.3(130265117-141098428), nine gains and only one loss were observed; thus, the further analysis so only focused on gain variants. The genes that may be related to invasion and metastasis in this region were *SH2D3C*, *ENG*, *CDK9*, *LRRC8A*, *VAV2*, *PPP1R26*, *EGFL7*, *EXD3*, *NRARP*, *RABL6*, *PTGDS*, *DDX31*, *SNHG7* and *CACNA1B*.

Among the regions with a gain in chromosome 17, arr17q21.31(44161441-44351452)x3, a systemic gain in DGV was commonly present and thus, it may be classified as a likely benign variant. Among the other gained regions, the genes that may be related to tumour progression and metastasis were *RTN4RL1*, *DOC2B*, *TBC1D3*, *MIEN1*, *GRB7*, *HOXB7*, *SPOP*, *DLX4*, *MIR454*, *ANKRD40C*L, *SPAG9*, *AKAP1*, *TRIM37*, *KPNA2*, *MAP2K6*, *SOX9* and *TNRC6C-AS1*.

In the gained region of chromosome 19, only *LILRB2* and *CNOT3* genes in arr19q13.42(54332068-54919859)x3 were indicated to be potentially related to cancer progression.

Certain genes detected in the regions with gains discussed above have already been reported to be involved in bladder

Table IV. Common CNV regions in bladder cancer samples.

Chromosome	Aberration	Number of samples	Cytobands	Start	Stop	Length (kb)	CNV change (-/+)
1	Ab. 1	5	p34.3p34.2	39548798	41088676	1539878	+
1	Ab. 2	4	p13.1p12	116361026	118042757	1681731	+
1	Ab. 3	5	q21.3	151271782	152259742	987960	+
1	Ab. 4	6	q23.2q23.3	160382554	162080328	1697775	+
1	Ab. 5	5	q31.3q32.1	198410156	201437832	3027676	+
2	Ab. 6	5	q11.2q12.2	102626416	107105269	4478853	+
2	Ab. 7	5	35q37.3	217186741	238597790	24990400	+
3	Ab. 8	5	q27.2q29	185131783	195623848	10492065	+
4	Ab. 9	5	p15.31p15.2	19047617	21526226	2478609	+
4	Ab. 10	5	p14	36317970	39459154	3141184	+
5	Ab. 11	5	p15.33p15.2	1159888	10124258	8964370	+
5	Ab. 12	6	p13.1p12	38542259	44812566	6270307	+
8	Ab. 13	5	p11.23p11.22	36778072	39223462	2445390	+
8	Ab. 14	6	q11.1q13.1	46923445	66409897	19486452	+
8	Ab. 15	6	q22.1q22.3	94359808	104577357	10217549	+
8	Ab. 16	5	q24.12q24.23	121918835	138034801	16115966	+
9	Ab. 7	4	p24.2p24.1	4483189	7324382	2841193	_
9	Ab. 18	5	p24.2p24.1	4483189	7324382	2841193	+
9	Ab. 19	5	p21.3	21746274	22004153	257879	-
9	Ab. 20	6	p21.3	21746274	22004153	257879	+
9	Ab. 21	2	q21.33q22.32	89345014	96677307	7332293	-
9	Ab. 22	4	q21.33q22.32	89345014	96677307	7332293	+
9	Ab. 23	1	q33.3q34.3	130265117	141098428	10833311	-
9	Ab. 24	9	q33.3q34.3	130265117	141098428	10833311	+
10	Ab. 25	6	p15.3p13	2291574	15075299	12783725	+
10	Ab. 26	6	p12.1p11.23	26530405	30212755	3682350	+
11	Ab. 27	6	q13.1q13.4	65782622	71287123	5504501	+
14	Ab. 28	5	q11.2q12	20652555	27002379	6349824	+
14	Ab. 29	6	q12q13.2	30527028	35537512	5010484	+
14	Ab. 30	5	q24.2q31.1	72962189	79510706	6548517	+
14	Ab. 31	6	q32.2	99762857	100398318	635461	+
17	Ab. 32	6	p13.3p13.2	13905	3676393	3662488	+
17	Ab. 33	6	q12	35958791	36593228	634437	+
17	Ab. 34	6	q12	37673211	38105334	432123	
17	Ab. 35	6	q21.31	44161441	44351452	190011	+
17	Ab. 36	6	q21.32q23.2	46545363	59277614	12732251	+
17	Ab. 37	5	q24.2q25.1	65584651	70979004	5394353	+
17	Ab. 38	5	q25.3	75816274	76303552	487278	+
19	Ab.39	5	q13.11	33013506	33370161	356655	+
19	Ab. 40	5	q13.42	54332068	54919859	587791	+
20	Ab. 41	6	p12.1	14715679	16003225	1287546	+
20	Ab. 42	7	p11.22p11.1	21559089	26285899	4726810	+
20	Ab. 43	8	q11.21	29530880	31803506	2272626	+
20	Ab. 44	8	q12q13.12	40678430	44278445	3600015	+
20	Ab. 45	8	q13.31	55804501	55957204	152703	+

-, losses and +, gains detected generally in more than four different bladder cancer samples, cytoband start and end position and length in kb. CNV, copy number variation; kb, kilobases

cancer genesis and progression. These genes included the following: *PFDN2* located on 1q23.3, detected in the urinary DNA with aCGH technique (21); *COL6A3* located in 2q37.3, which promotes epithelial-mesenchymal transition in bladder

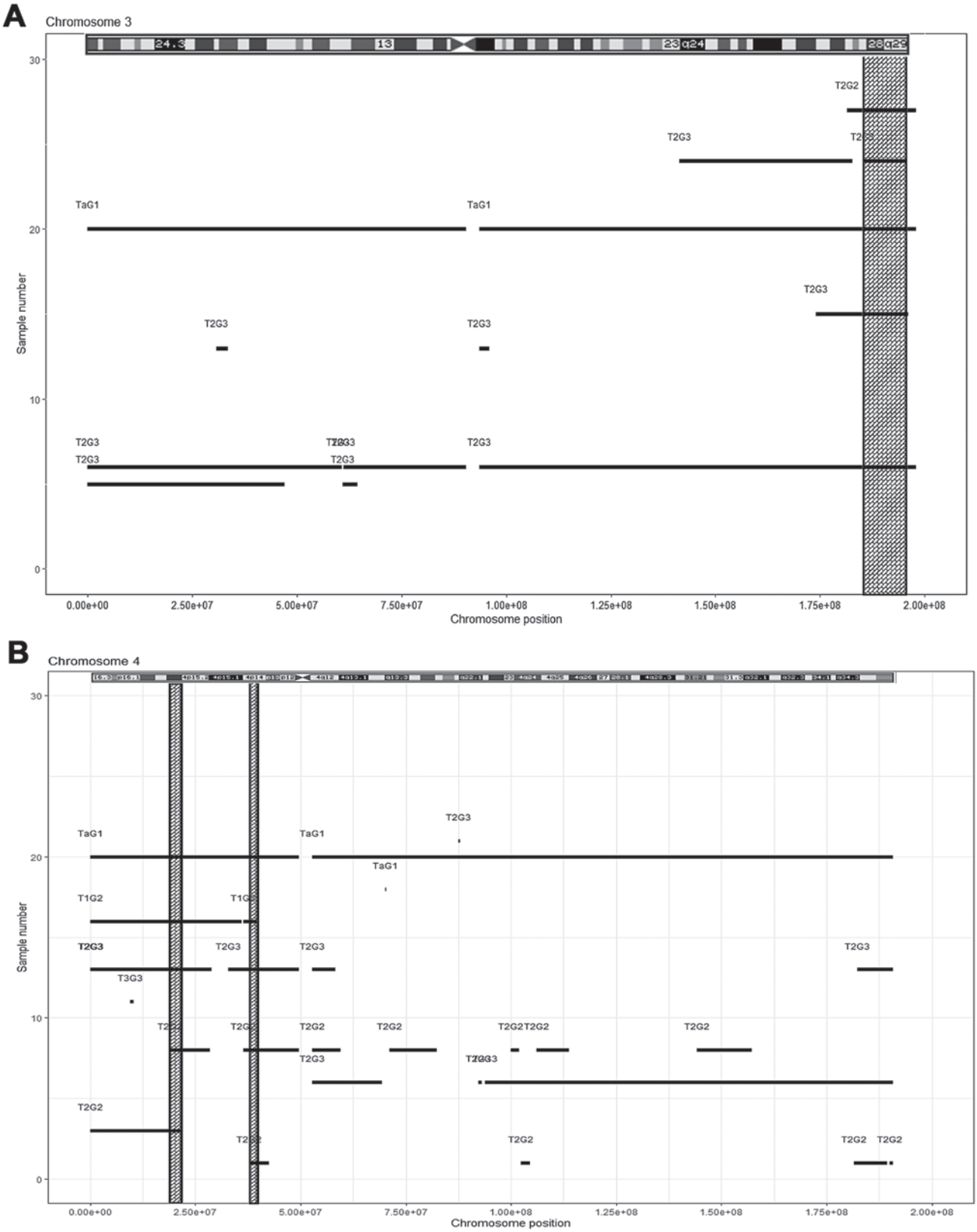

Figure 3. CNVs detected in (A) chromosome 3 and (B) chromosome 4. X-axis indicates the genomic position and the Y-axis indicates individual tumour samples tested. Chromosomal regions with again are indicated with a black straight line. No losses were detected. The shaded vertical fields indicate the start and the end of each CNV overlapping in at least five tumours. CNV, copy number variation.

cancer cells via the TGF-β/Smad pathway (22); *DNER* in 2q36.3, involved in proliferation, migration and invasion by regulating the activation of the PI3K/AKT pathway (23). *OSMR* in 5p13.1 was indicated to be closely associated with cell growth and differentiation, inflammation and enhancement of metastatic capacity in urinary bladder cancer (24).

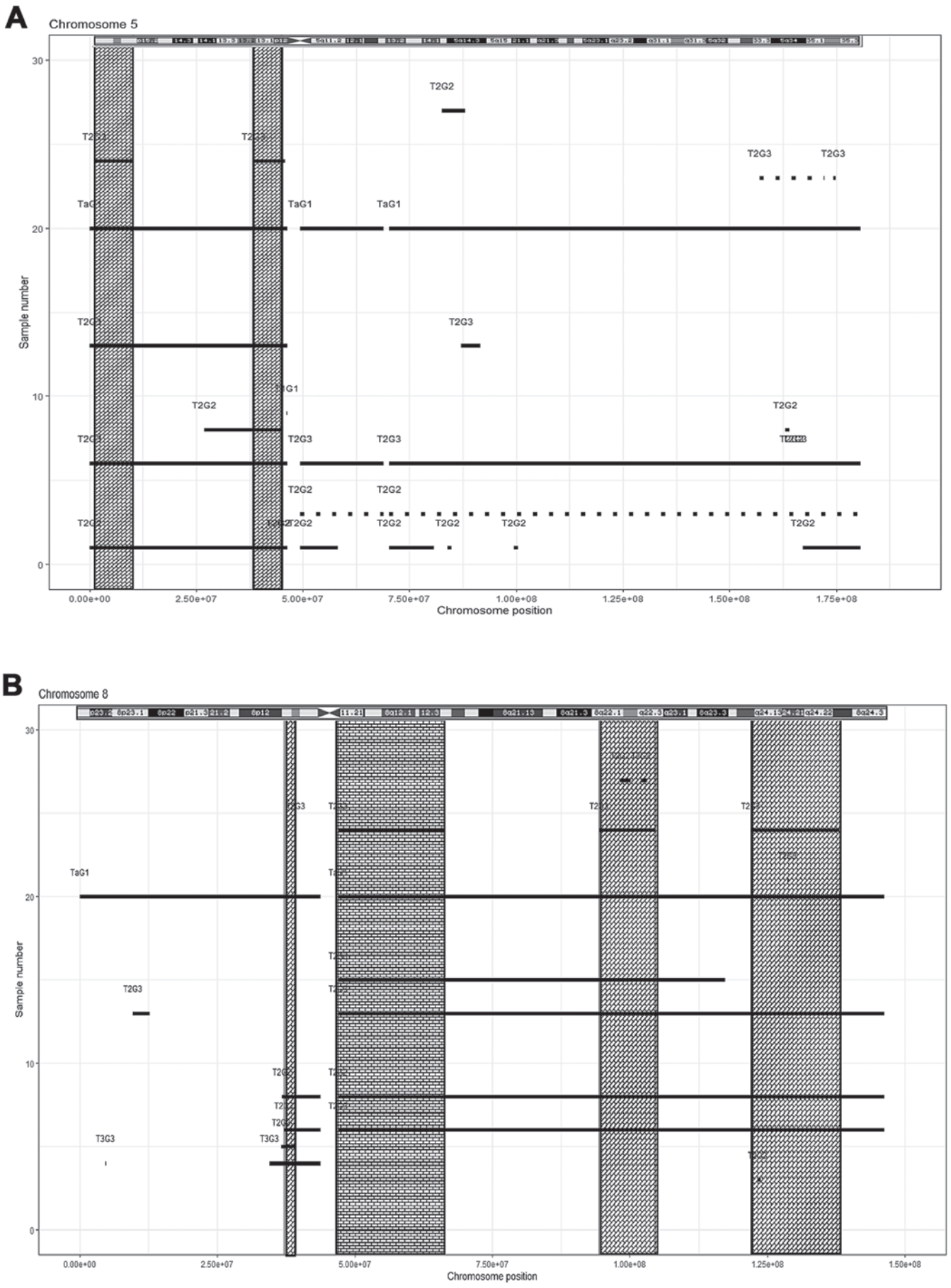

Figure 4. CNVs detected in (A) chromosome 5 and (B) chromosome 8. X-axis indicates the genomic position and the Y-axis indicates individual tumour samples tested. Chromosomal regions with gain are indicated with a black straight line and chromosomal regions with losses are displayed with a black dotted line. The shaded vertical fields indicate the start and the end of each CNV overlapping in at least five tumours. CNV, copy number variation.

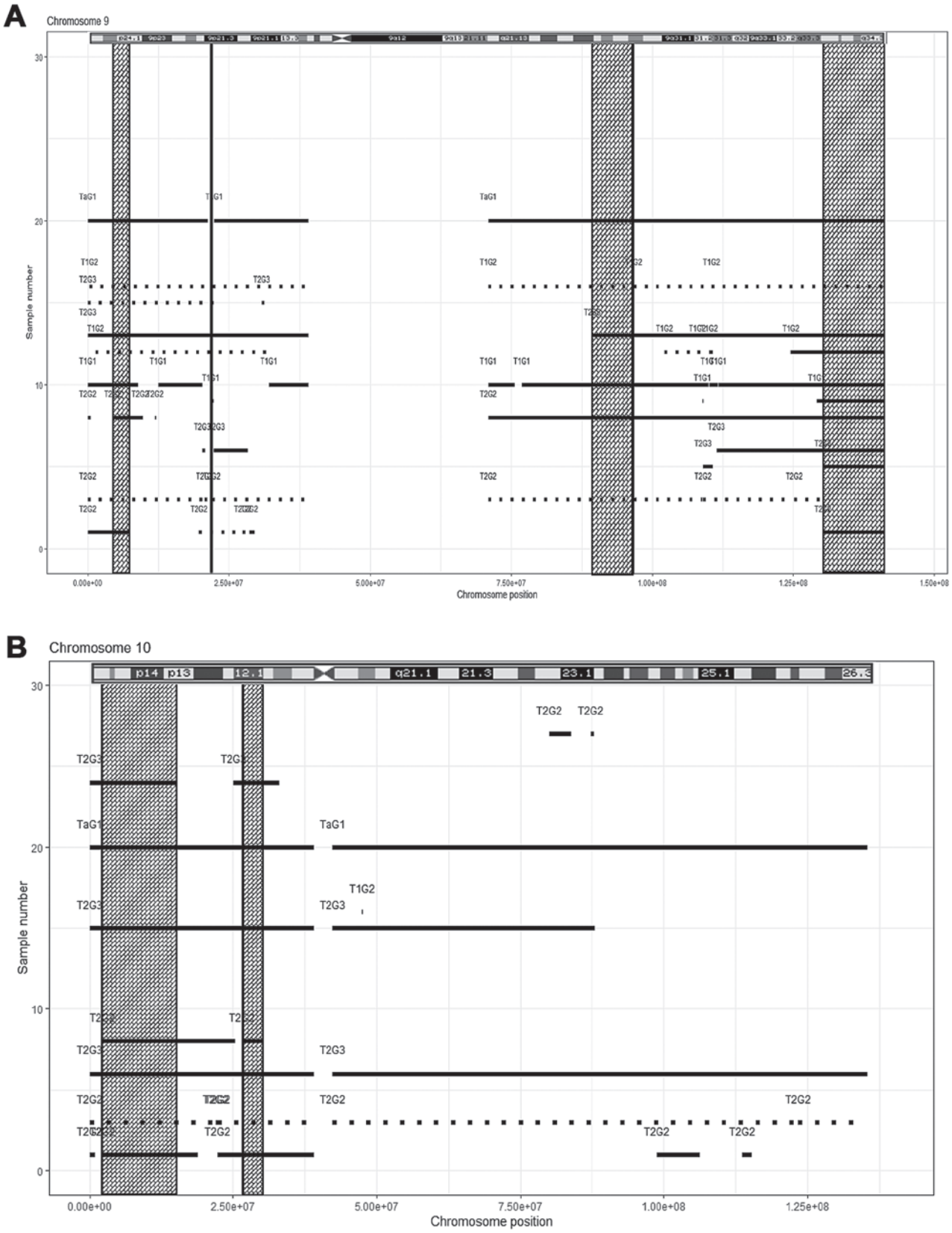

Figure 5. CNVs detected in (A) chromosome 9 and (B) chromosome 10. X-axis indicates the genomic position and the Y-axis indicates individual tumour samples tested. Chromosomal regions with gain are indicated with a black straight line and chromosomal regions with losses are displayed with a black dotted line. The shaded vertical fields indicate the start and the end of each CNV overlapping in more than five tumours. CNV, copy number variation.

MYC, located in 8q24.21, has been reported in numerous studies to be involved in cell growth and migration in bladder cancer (25). Genes *DDX31* and *SNHG7*, which are oncogenes that have been reported to be dysregulated in various tumour types, have also been previously indicated to be involved in bladder cancer metastases (26,27). Both are located

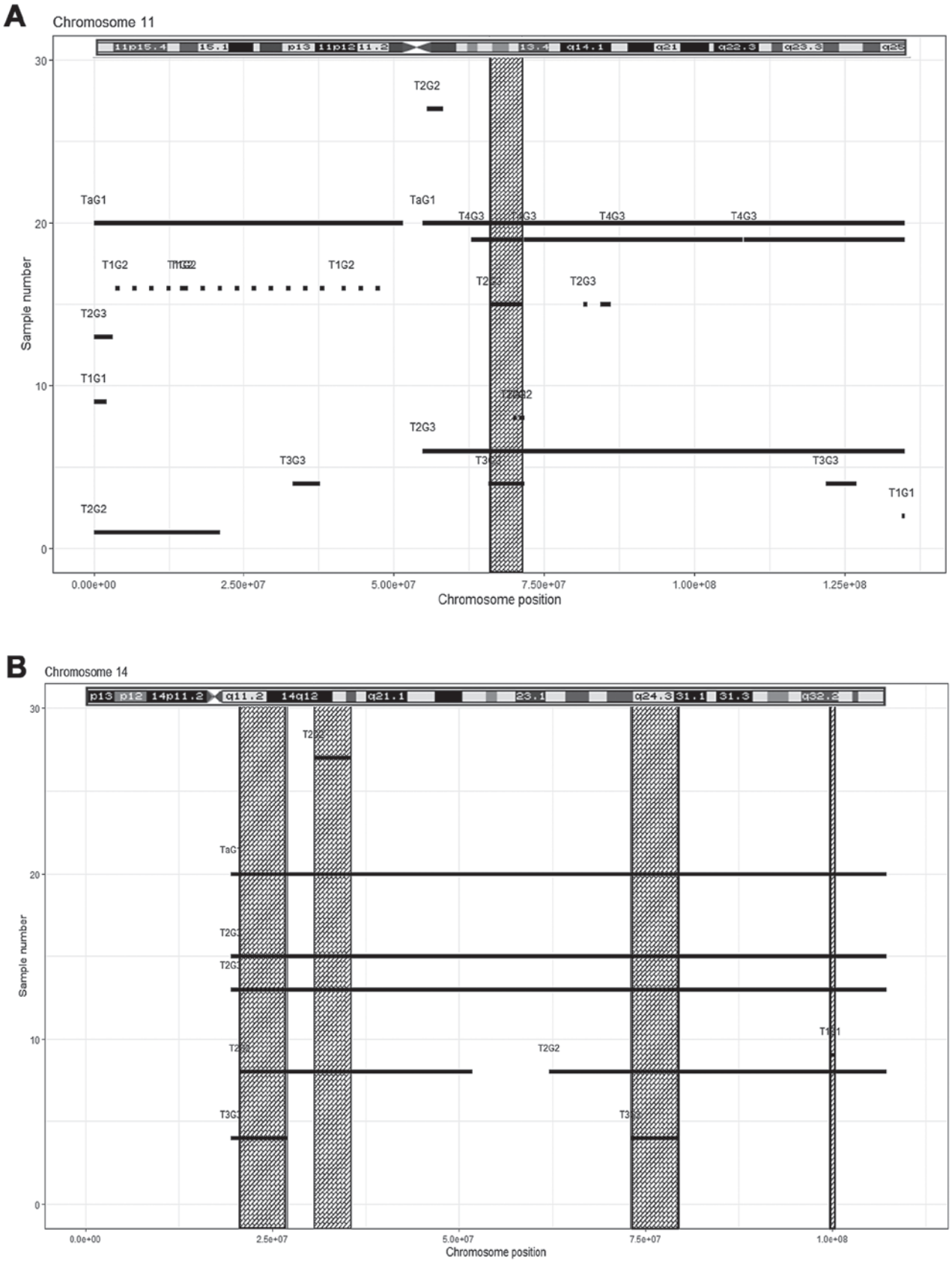

Figure 6. CNVs detected in (A) chromosome 11 and (B) chromosome 14. X-axis indicates the genomic position and the Y-axis indicates individual tumour samples tested. Chromosomal regions with gain are indicated with a black straight line and chromosomal regions with losses are displayed with a black dotted line. The shaded vertical fields indicate the start and the end of each CNV overlapping more than five tumours. CNV, copy number variation.

in the 'gain' chromosomal region in the terminal end of chromosome 9, arr9q33.3q34.3(130265117-141098428). The *SLC39A11* located in 17q24.3-q25.1 has been reported to be associated with survival of patients with bladder cancer (28).

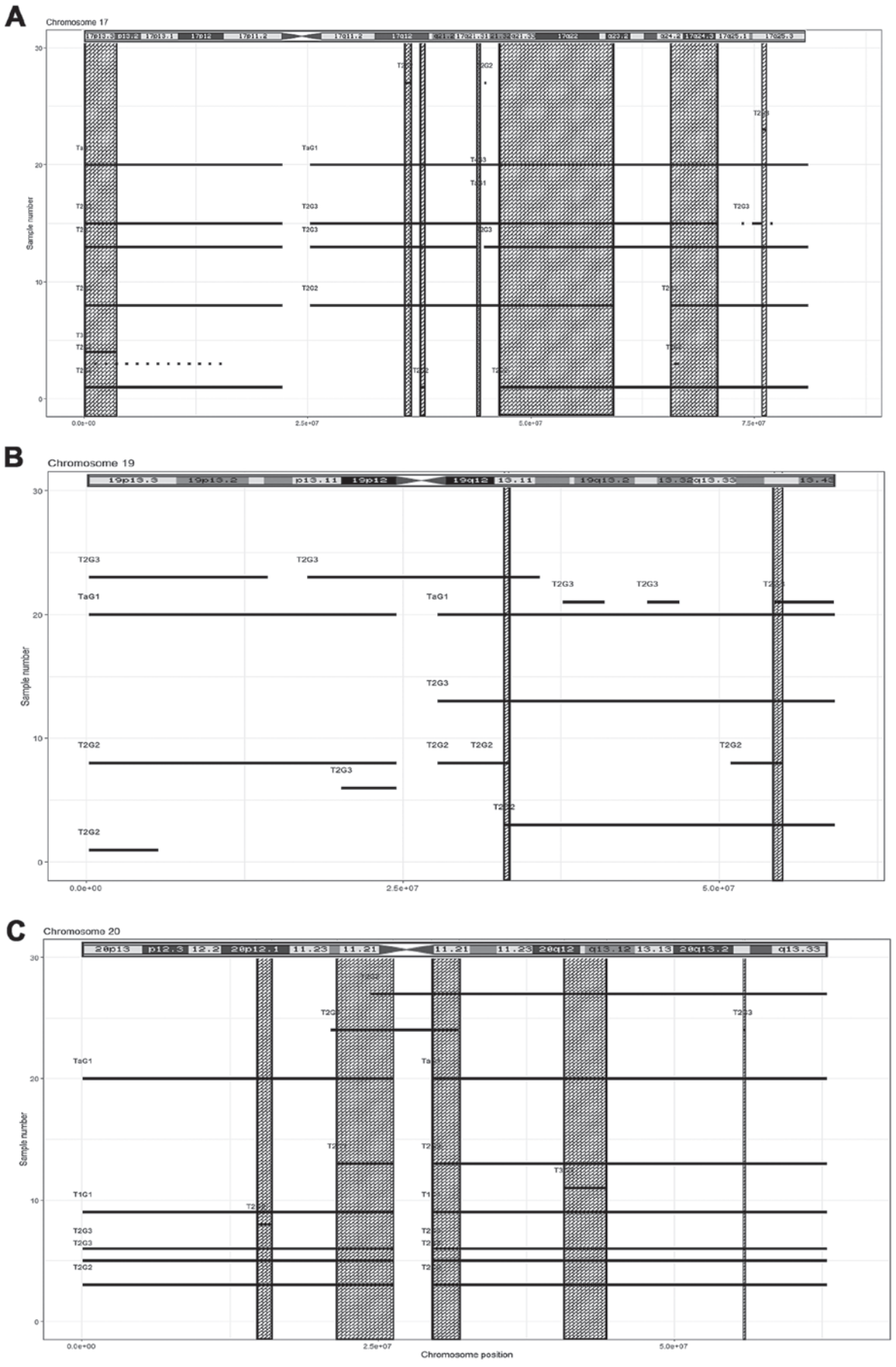

Figure 7. CNVs detected in (A) chromosome 17 and (B) chromosome 19 and (C) chromosome 20. X-axis indicates the genomic position and the Y-axis indicates individual tumour samples tested. Chromosomal regions with gain are indicated with a black straight line and chromosomal regions with losses are displayed with a black dotted line. The shaded vertical fields indicate the start and the end of each CNV overlapping more than four tumours. CNV, copy number variation.

Table V. Genes related to cancer invasion and metastasis among the common gain pathogenic variant.

Array	Gene name (gene symbol)
arr1p34.3p34.2(39548798-41088676)x3	Microtubule actin crosslinking factor 1 (*MACF1*)
arr1p34.3p34.2(39548798-41088676)x3	L-myc-1 proto-oncogene (*MYCL*)
arr1p34.3p34.2(39548798-41088676)x3	Basic helix-loop-helix (*bHLH*)
arr1p34.3p34.2(39548798-41088676)x3	Hes-related family bHLH transcription factor (*HEYL*)
arr1p13.1p12(116361026-118042757)x3	Prostaglandin F2 receptor inhibitor (*PTGFRN*)
arr1q21.3(151271782-152259742)x3	S100 calcium binding protein A1 (*S100A1*)
arr1q21.3(151271782-152259742)x3	Hornerin (*HRNR*)
arr1q21.3(151271782-152259742)x3	Regulatory factor X5 (*RFX5*)
arr1q21.3(151271782-152259742)x3	Proteasome 20S subunit beta 4p (*PSMB4*)
arr1q23.2q23.3(160382554-162080328)x3	Nectin cell adhesion molecule 4 (*NECTIN4*)
arr1q23.2q23.3(160382554-162080328)x3	Beta-1,4-galactosyltransferase 3 (*B4GALT3*)
arr1q23.2q23.3(160382554-162080328)x3	Olfactomedin like 2B (*OLFML2B*)
arr1q31.3q32.1(198410156-201437832)x3	Ladinin 1 (*LAD1*)
arr1q31.3q32.1(198410156-201437832)x3	Nuclear receptor subfamily 5 group A member 2 (*NR5A2*)
arr1q31.3q32.1(198410156-201437832)x3	Kinesin family member 14 (*KIF14*)
arr2q11.2q12.2(102626416-107105269)x3	POU class 3 homeobox 3 (*POU3F3*)
arr2q11.2q12.2(102626416-107105269)x3	Four and a half LIM domains 2 (*FHL2*)
arr2q11.2q12.2(102626416-107105269)x3	NCK adaptor protein 2 (*NCK2*)
arr2q35q37.3(217186741-238597790)x3	Wnt family member 6 (*WNT6*)
arr2q35q37.3(217186741-238597790)x3	CCR4-NOT transcription complex subunit 9 (*CNOT9*)
arr2q35q37.3(217186741-238597790)x3	Serine/threonine kinase 16 (*STK16*)
arr2q35q37.3(217186741-238597790)x3	Actin related protein 2/3 complex subunit 2 (*ARPC2*)
arr2q35q37.3(217186741-238597790)x3	Disrupted in renal carcinoma 3 (*DIRC3*)
arr2q35q37.3(217186741-238597790)x3	EPH receptor A4 (*EPHA4*)
arr2q35q37.3(217186741-238597790)x3	Paired box 3 (*PAX3*)
arr2q35q37.3(217186741-238597790)x3	Serpin family E member 2 (*SERPINE2*)
arr2q35q37.3(217186741-238597790)x3	ADP ribosylation factor like GTPase 4C (*ARL4C*)
arr3q27.2q29(185131783-195623848)x3	Mitogen-activated protein kinase kinase kinase 13 (*MAP3K13*)
arr3q27.2q29(185131783-195623848)x3	Insulin like growth factor 2 mRNA binding protein 2 (*IGF2BP2*)
arr3q27.2q29(185131783-195623848)x3	Transformer 2 beta homolog (*TRA2B*)
arr3q27.2q29(185131783-195623848)x3	Replication factor C subunit 4 (*RFC4*)
arr3q27.2q29(185131783-195623848)x3	Ribosomal protein L39 like (*RPL39L*)
arr3q27.2q29(185131783-195623848)x3	BCL6 transcription repressor (*BCL6*)
arr3q27.2q29(185131783-195623848)x3	MicroRNA 944 (*MIR944*)
arr3q27.2q29(185131783-195623848)x3	MicroRNA 5692c-1 (*MIR5692C1*)
arr3q27.2q29(185131783-195623848)x3	Hes family bHLH transcription factor 1 (*HES1*)
arr3q27.2q29(185131783-195623848)x3	Carboxypeptidase N subunit 2 (*CPN2*)
arr4p15.31p15.2(19047617-21526226)x3	MicroRNA 218-1 (*MIR218-1*)
arr4p14(36317970–39459154)x3	Toll like receptor 6 (*TLR6*)
arr5p15.33p15.2(1159888–10124258)x3	CLPTM1 like (*CLPTM1L*)
arr5p15.33p15.2(1159888–10124258)x3	Iroquois homeobox 2 (*IRX2*)
arr5p13.1p12(38542259-44812566)x3	Oncostatin M receptor (*OSMR*)
arr5p13.1p12(38542259-44812566)x3	Poly(A) binding protein interacting protein 1 (*PAIP1*)
arr5p13.1p12(38542259-44812566)x3	Chromosome 5 open reading frame 34 (*C5orf34*)
arr5p13.1p12(38542259-44812566)x3	Nicotinamide nucleotide transhydrogenase (*NNT*)
arr8p11.23p11.22(36778072-39223462)x3	Phospholipid phosphatase 5 (*PLPP5*)
arr8p11.23p11.22(36778072-39223462)x3	BAG cochaperone 4 (*BAG4*)
arr8q11.1q13.1(46923445-66409897)x3	CCAAT enhancer binding protein delta (*CEBPD*)
arr8q11.1q13.1(46923445-66409897)x3	Lysophospholipase 1 (*LYPLA1*)
arr8q11.1q13.1(46923445-66409897)x3	Long intergenic non-protein coding RNA 1606 (*LINC01606*)
arr8q11.1q13.1(46923445-66409897)x3	MIR124-2 host gene (*MIR124-2HG*)
arr8q11.1q13.1(46923445-66409897)x3	Syndecan binding protein (*SDCBP*)

Table V. Continued.

Array	Gene name (gene symbol)
arr8q22.1q22.3(94359808-104577357)x3	MicroRNA 5680 (*MIR5680*)
arr8q22.1q22.3(94359808-104577357)x3	Collagen triple helix repeat containing 1 (*CTHRC1*)
arr8q24.12q24.23(121918835-138034801)x3	Hyaluronan synthase 2 (*HAS2*)
arr8q24.12q24.23(121918835-138034801)x3	Annexin A13 (*ANXA13*)
arr8q24.12q24.23(121918835-138034801)x3	NADH:ubiquinone oxidoreductase subunit B9 (*NDUFB9*)
arr9q33.3q34.3(130265117-141098428)x3	SH2 domain containing 3C (*SH2D3C*)
arr9q33.3q34.3(130265117-141098428)x3	Endoglin (*ENG*)
arr9q33.3q34.3(130265117-141098428)x3	Cyclin dependent kinase 9 (*CDK9*)
arr9q33.3q34.3(130265117-141098428)x3	Leucine rich repeat containing 8 subunit A (*LRRC8A*)
arr9q33.3q34.3(130265117-141098428)x3	Vav guanine nucleotide exchange factor 2 (*VAV2*)
arr9q33.3q34.3(130265117-141098428)x3	Protein phosphatase 1 regulatory subunit 26 (*PPP1R26*)
arr9q33.3q34.3(130265117-141098428)x3	EGF like domain multiple 7 (*EGFL7*)
arr9q33.3q34.3(130265117-141098428)x3	Exonuclease 3'-5' domain containing 3 (*EXD3*)
arr9q33.3q34.3(130265117-141098428)x3	NOTCH regulated ankyrin repeat protein (*NRARP*)
arr9q33.3q34.3(130265117-141098428)x3	RAB, member RAS oncogene family like 6 (*RABL6*)
arr9q33.3q34.3(130265117-141098428)x3	Prostaglandin D2 synthase (*PTGDS*)
arr9q33.3q34.3(130265117-141098428)x3	Calcium voltage-gated channel subunit alpha1 B (*ACNA1B*)
arr9q33.3q34.3(130265117-141098428)x3	DEAD-box helicase 31 (*DDX31*)
arr9q33.3q34.3(130265117-141098428)x3	Small nucleolar RNA host gene 7 (*SNHG7*)
arr10p15.3p13(2291574-15075299)x3	Kruppel like factor 6 (*KLF6*)
arr10p15.3p13(2291574-15075299)x3	RNA binding motif protein 17 (*RBM17*)
arr10p15.3p13(2291574-15075299)x3	6-phosphofructo-2-kinase/fructose-2,6-biphosphatase 3 (*PFKFB3*)
arr10p15.3p13(2291574-15075299)x3	Kin17 DNA and RNA binding protein (*KIN*)
arr10p12.1p11.23(26530405-30212755)x3	Microtubule associated serine/threonine kinase like (*MASTL*)
arr11q13.1q13.4(65782622-71287123)x3	Carnitine palmitoyltransferase 1A (*CPT1A*)
arr11q13.1q13.4(65782622-71287123)x3	MAS related GPR family member D (*MRGPRD*)
arr11q13.1q13.4(65782622-71287123)x3	Fibroblast growth factor 3 (*FGF3*)
arr11q13.1q13.4(65782622-71287123)x3	Fibroblast growth factor 4 (*FGF4*)
arr14q11.2q12(20652555-27002379)	NDRG family member 2 (*NDRG2*)
arr14q11.2q12(20652555-27002379)	Methyltransferase like 3 (*METTL3*)
arr14q11.2q12(20652555-27002379)	Chromodomain helicase DNA binding protein 8 (*CHD8*)
arr14q11.2q12(20652555-27002379)	Proteasome 20S subunit beta 5 (*PSMB5*)
arr14q11.2q12(20652555-27002379)	Protein arginine methyltransferase 5 (*PRMT5*)
arr14q11.2q12(20652555-27002379)	DDB1 and CUL4 associated factor 11 (*DCAF11*)
arr14q12q13.2(30527028-35537512)x3	Egl-9 family hypoxia inducible factor 3 (*EGLN3*)
arr14q12q13.2(30527028-35537512)x3	Sorting nexin 6 (*SNX6*)
arr14q24.2q31.1(72962189-79510706)x3	PNMA family member 1 (*PNMA1*)
arr14q24.2q31.1(72962189-79510706)x3	Activator of HSP90 ATPase activity 1 (*AHSA1*)
arr14q32.2(99762857-100398318)x3	MicroRNA 5698 (*MIR5698*)
arr 17p13.3p13.2(13905-3676393)x3	Reticulon 4 receptor like 1 (*RTN4RL1*)
arr 17p13.3p13.2(13905-3676393)x3	Rouble C2 domain beta (*DOC2B*)
arr17q12(35958791-36593228)x3	TBC1 domain family member 3 (*TBC1D3*)
arr17q12(37673211-38105334)x3	Migration and invasion enhancer 1 (*MIEN1*)
arr17q12(37673211-38105334)x3	Growth factor receptor bound protein 7 (*GRB7*)
arr17q21.32q23.2(46545363-59277614)x3	Homeobox B7 (*HOXB7*)
arr17q21.32q23.2(46545363-59277614)x3	Speckle type BTB/POZ protein (*SPOP*)
arr17q21.32q23.2(46545363-59277614)x3	Distal-less homeobox 4 (*DLX4*)
arr17q21.32q23.2(46545363-59277614)x3	MicroRNA 454 (*MIR454*)
arr17q21.32q23.2(46545363-59277614)x3	ANKRD40 C-terminal like (*ANKRD40CL*)
arr17q21.32q23.2(46545363-59277614)x3	Sperm associated antigen 9 (*SPAG9*)
arr17q21.32q23.2(46545363-59277614)x3	A-kinase anchoring protein 1 (*AKAP1*)
arr17q21.32q23.2(46545363-59277614)x3	Tripartite motif containing 37 (*TRIM37*)

Table V. Continued.

Array	Gene name (gene symbol)
arr17q24.2q25.1(65584651-70979004)x3	Karyopherin subunit alpha 2 (*KPNA2*)
arr17q24.2q25.1(65584651-70979004)x3	Mitogen-activated protein kinase kinase 6 (*MAP2K6*)
arr17q24.2q25.1(65584651-70979004)x3	AS1 SOX9 antisense RNA 1 (*SOX9*)
arr17q25.3(75816274-76303552)x3	TNRC6C antisense RNA 1 (*TNRC6C-AS1*)
19q13.42(54332068-54919859)x3	Leukocyte immunoglobulin like receptor B2 (*LILRB2*)
19q13.42(54332068-54919859)x3	CCR4-NOT transcription complex subunit 3 (*CNOT3*)
arr20p12.1(14715679-16003225)x3	Mono-ADP ribosylhydrolase 2 (*MACROD2*)
arr20p11.22p11.1(21559089-26285899)x3	Ninein like (*NINL*)
arr20p11.22p11.1(21559089-26285899)x3	GINS complex subunit 1 (*GINS1*)
arr20q11.21(29530880-31803506)x3	PLAG1 like zinc finger 2 (*PLAGL2*)
arr20q12q13.12(40678430-44278445)x3	Serine and arginine rich splicing factor 6 (*SRSF6*)
arr20q12q13.12(40678430-44278445)x3	Semenogelin 1 (*SEMG1*)
arr20q12q13.12(40678430-44278445)x3	Translocase of outer mitochondrial membrane 34 (*TOMM34*)
arr20q13.31(55804501-55957204)x3	Ribonucleic acid export 1 (*RAE1*)

The table lists the genes related to cancer invasion and metastasis from the recurrent gain pathogenic copy number variation regions (described in Table III) common in more than four bladder cancer samples.

The enhanced methylation status of PRAC1 in 17q21.32 has been linked to a high recurrence rate and progression in patients with bladder cancer (29). Chen *et al* (30) indicated that the *KAT7* in 17q21.33, promotes cell proliferation in bladder cancer samples.

The genes detected in the LOH regions may be investigated in further studies and functional analyses regarding their potential tumour-suppressor role may be performed.

One limitation of the present study is the small sample size. However, even in this small cohort, a large quantity of aberrations were detected, which are difficult to classify without any strict statistical, histological and bioinformatical criteria, which unfortunately have not yet been developed. Additionally, a relatively small sample cohort may lead to statistical errors with overrepresentation of certain aberrations and therefore, the prevalence rate of particular chromosomal aberrations may not be representative of bladder cancer imbalances in general. Another limitation of the study is that the analysis of genomic imbalances was performed at the DNA level only, so the next step should be gene expression analysis or functional investigation of identified genes that have not already been reported elsewhere to be involved in bladder cancer. Despite the limitations of the present study, the results obtained are of significant scientific value, as they provide certain mechanisms that may be responsible for tumour invasion caused by genetic imbalances related to the activation of genes with metastatic and proliferative potential. A total of 42 recurrent CNVs, mostly in high-grade bladder tumours, were detected in chromosomes 1-5, 8-11, 14, 17, 19 and 20. Furthermore, in the present study, genes potentially related to the metastatic potential of uroepithelial tumours were identified that may be further studied as possible targets for precision therapy. Finally, five LOH variants in high-grade bladder cancer tumours were described.

In conclusion, the present study demonstrated that applying genomic approaches to bladder cancer research is crucial for furthering the current knowledge on the progression of the disease and the inclusion of these technologies as part of routine patient care, thus accelerating the implementation of a personalized therapeutic approach.

Acknowledgements

Bulgarian Ministry of Education and Science under the National Program for Research 'Young Scientists and Postdocotral Students'.

Funding

This work was funded by the Bulgarian Ministry of Education (grant no. DM13/4, 2017) and the Medical University of Sofia (grant no. D-60/03.05.2018).

Availability of data and materials

The datasets used and/or analysed during the current study are available from the corresponding author on reasonable request.

Authors' contributions

OA was involved in the conception of the study, sample processing and writing of the manuscript. BM, SR and CS were involved in tumour sample collection. ZH and DN were involved in DNA isolation. LB, RV and SH were involved in CNV detection. VS and MG analysed the data and prepared the figures. DS and RS were involved in statistical analyses. DT was involved in study design and manuscript revision. OA, LB and RV confirm the authenticity of all the raw data. All the authors read and approved the final version of the manuscript.

Ethics approval and consent to participate

This study was approved by the Ethical Committee of the Medical University of Sofia (Sofia, Bulgaria; protocol no. 04/09/03/2018). Written informed consent was obtained from the participants prior to tissue collection.

Patient consent for publication

Not applicable.

Competing interests

The authors declare that they have no competing interests.

References

1. Conconi D, Panzeri E, Redaelli S, Bovo G, Viganò P, Strada G, Dalprà L and Bentivegna A: Chromosomal imbalances in human bladder urothelial carcinoma: Similarities and differences between biopsy samples and cancer stem-like cells. BMC Cancer 14: 646, 2014.
2. Kawanishi H, Takahashi T, Ito M, Matsui Y, Watanabe J, Ito N, Kamoto T, Kadowaki T, Tsujimoto G, Imoto I, *et al*: Genetic analysis of multifocal superficial urothelial cancers by array-based comparative genomic hybridisation. Br J Cancer 97: 260-266, 2007
3. Kallioniemi A, Kallioniemi OP, Citro G, Sauter G, DeVries S, Kerschmann R, Caroll P and Waldman F: Identification of gains and losses of DNA sequences in primary bladder cancer by comparative genomic hybridization. Genes Chromosomes Cancer 12: 213-219, 1995.
4. Sauter G: Rudolf Virchow Prize 1997. Molecular cytogenetic analysis of superficial urothelial cancer of the bladder. Verh Dtsch Ges Pathol 81: 18-27, 1997 (In German).
5. Voorter C, Joos S, Bringuier PP, Vallinga M, Poddighe P, Schalken J, du Manoir S, Ramaekers F, Lichter P and Hopman A: Detection of chromosomal imbalances in transitional cell carcinoma of the bladder by comparative genomic hybridization. Am J Pathol 146: 1341-1354, 1995.
6. Zaharieva BM, Simon R, Diener PA, Ackermann D, Maurer R, Alund G, Knönagel H, Rist M, Wilber K, Hering F, *et al*: High-throughput tissue microarray analysis of 11q13 gene amplification (CCND1, FGF3, FGF4, EMS1) in urinary bladder cancer. J Pathol 201: 603-608, 2003.
7. Huang WC, Taylor S, Nguyen TB, Tomaszewski JE, Libertino JA, Malkowicz SB and McGarvey TW: KIAA1096, a gene on chromosome 1q, is amplified and overexpressed in bladder cancer. DNA Cell Biol 21: 707-715, 2002.
8. Veltman JA, Fridlyand J, Pejavar S, Olshen AB, Korkola JE, DeVries S, Carroll P, Kuo WL, Pinkel D, Albertson D, *et al*: Array-based comparative genomic hybridization for genome-wide screening of DNA copy number in bladder tumors. Cancer Res 63: 2872-2880, 2003.
9. Bellmunt J, Selvarajah S, Rodig S, Salido M, de Muga S, Costa I, Bellosillo B, Werner L, Mullane S, Fay AP, *et al*: Identification of ALK gene alterations in urothelial carcinoma. PLoS One 9: e103325, 2014.
10. Scaravilli M, Asero P, Tammela TL, Visakorpi T and Saramäki OR: Mapping of the chromosomal amplification 1p21-22 in bladder cancer. BMC Res Notes 7: 547, 2014.
11. Weilandt M, Koch A, Rieder H, Deenen R, Schwender H, Niegisch G and Schulz WA: Target genes of recurrent chromosomal amplification and deletion in urothelial carcinoma. Cancer Genomics Proteomics 11: 141-153, 2014.
12. Ewald JA, Downs TM, Cetnar JP and Ricke WA: Expression microarray meta-analysis identifies genes associated with Ras/MAPK and related pathways in progression of muscle-invasive bladder transition cell carcinoma. PLoS One 8: e55414, 2013.
13. Hussain SA, Palmer DH, Syn WK, Sacco JJ, Greensmith RM, Elmetwali T, Aachi V, Lloyd BH, Jithesh PV, Arrand J, *et al*: Gene expression profiling in bladder cancer identifies potential therapeutic targets. Int J Oncol 50: 1147-1159, 2017.
14. Mengual L, Burset M, Ars E, Lozano JJ, Villavicencio H, Ribal MJ and Alcaraz A: DNA microarray expression profiling of bladder cancer allows identification of noninvasive diagnostic markers. J Urol 182: 741-748, 2009.
15. Sanchez-Carbayo M: Use of high-throughput DNA microarrays to identify biomarkers for bladder cancer. Clin Chem 49: 23-31, 2003.
16. de Ravel TJ, Devriendt K, Fryns JP and Vermeesch JR: What's new in karyotyping? The move towards array comparative genomic hybridisation (CGH). Eur J Pediatr 166: 637-643, 2007.
17. Letasiova S, Medve'ova A, Sovcikova A, Dušinská M, Volkovová K, Mosoiu C and Bartonová A: Bladder cancer, a review of the environmental risk factors. Environ Health 11 Suppl 1(Suppl 1): S11, 2012.
18. Minner S, Kilgue A, Stahl P, Weikert S, Rink M, Dahlem R, Fisch M, Höppner W, Wagner W, Bokemeyer C, *et al*: Y chromosome loss is a frequent early event in urothelial bladder cancer. Pathology 42: 356-359, 2010.
19. Panani AD and Roussos C: Sex chromosome abnormalities in bladder cancer: Y polysomies are linked to PT1-grade III transitional cell carcinoma. Anticancer Res 26(1A): 319-323, 2006.
20. Forsberg LA: Loss of chromosome Y (LOY) in blood cells is associated with increased risk for disease and mortality in aging men. Hum Genet 136: 657-663, 2017.
21. Lopez V, Gonzalez-Peramato P, Suela J, Serrano A, Algaba F, Cigudosa JC, Vidal A, Bellmunt J, Heredero O and Sánchez-Carbayo M: Identification of prefoldin amplification (1q23.3-q24.1) in bladder cancer using comparative genomic hybridization (CGH) arrays of urinary DNA. J Transl Med 11: 182, 2013.
22. Huang Y, Li G, Wang K, Mu Z, Xie Q, Qu H, Lv H and Hu B: Collagen Type VI Alpha 3 Chain promotes epithelial-mesenchymal transition in bladder cancer cells via transforming growth factor β (TGF-β)/Smad pathway. Med Sci Monit 24: 5346-5354, 2018.
23. Liang Y, Luo H, Zhang H, Dong Y and Bao Y: Oncogene Delta/Notch-Like EGF-Related receptor promotes cell proliferation, invasion, and migration in hepatocellular carcinoma and predicts a poor prognosis. Cancer Biother Radiopharm 33: 380-386, 2018.
24. Deng S, He SY, Zhao P and Zhang P: The role of oncostatin M receptor gene polymorphisms in bladder cancer. World J Surg Oncol 17: 30, 2019.
25. Sun J, Zhang H, Tao D, Xie F, Liu F, Gu C, Wang M, Wang L, Jiang G, Wang Z and Xiao X: CircCDYL inhibits the expression of C-MYC to suppress cell growth and migration in bladder cancer. Artif Cells Nanomed Biotechnol 47: 1349-1356, 2019.
26. Chen Y, Peng Y, Xu Z, Ge B, Xiang X, Zhang T, Gao L, Shi H, Wang C and Huang J: Knockdown of lncRNA SNHG7 inhibited cell proliferation and migration in bladder cancer through activating Wnt/β-catenin pathway. Pathol Res Pract 215: 302-307, 2019.
27. Daizumoto K, Yoshimaru T, Matsushita Y, Fukawa T, Uehara H, Ono M, Komatsu M, Kanayama HO and Katagiri T: A DDX31/Mutant-p53/EGFR Axis promotes multistep progression of Muscle-Invasive bladder cancer. Cancer Res 78: 2233-2247, 2018.
28. Wu L, Chaffee KG, Parker AS, Sicotte H and Petersen GM: Zinc transporter genes and urological cancers: Integrated analysis suggests a role for ZIP11 in bladder cancer. Tumour Biol 36: 7431-7437, 2015.
29. Kim YW, Yoon HY, Seo SP, Lee SK, Kang HW, Kim WT, Bang HJ, Ryu DH, Yun SJ, Lee SC, *et al*: Clinical implications and prognostic values of prostate cancer susceptibility candidate methylation in primary nonmuscle invasive bladder cancer. Dis Markers 2015: 402963, 2015.
30. Chen Z, Zhou L, Wang L, Kazobinka G, Zhang X, Han X, Li B and Hou T: HBO1 promotes cell proliferation in bladder cancer via activation of Wnt/β-catenin signaling. Mol Carcinog 57: 12-21, 2018.